EARTHQUAKE ENGINEERING AND STRUCTURAL DYNAMICS
Earthquake Engng Struct. Dyn. 2002; **31**:1915–1932 (DOI: 10.1002/eqe.195)

Seismic response analysis on the stability of running vehicles

Yoshihisa Maruyama[1,*,†] and Fumio Yamazaki[2]

[1] *Institute of Industrial Science, The University of Tokyo, 4-6-1 Komaba, Meguro-ku, Tokyo 153-8505, Japan*
[2] *Asian Institute of Technology, Pathumthani 12120, Thailand*

SUMMARY

The seismometer network of the Japanese expressway system has been enhanced since the 1995 Kobe earthquake. Using earthquake information from the instruments, the expressways are closed if the peak ground acceleration (PGA) is larger than or equal to 80 cm/s^2. The aim of this regulation is to avoid secondary disasters, e.g. cars running into the collapsed sections. However, recent studies on earthquake damage have revealed that expressway structures are not seriously damaged under such-level of earthquake motion. Hence, we may think of relaxing the regulation of expressway closure. But before doing this, it is necessary to examine the effects of shaking to automobiles since the drivers may encounter difficulties in controlling their vehicles and traffic accidents may occur. In this study, a vehicle was modelled with a six-degree-of-freedom system and its responses were investigated with respect to PGA, peak ground velocity (PGV) and Japan Meteorological Agency (JMA) seismic intensity using five ground motion records. It was observed that the response of the vehicle shows a larger amplitude for the record that has larger response spectrum in the long period range compared to other records. However, similar response amplitudes of the vehicle were observed for all the records with respect to the JMA seismic intensity. The response characteristics of the vehicle model may be very useful for decision-making regarding the relaxation of the expressway closure under seismic motion. Copyright © 2002 John Wiley & Sons, Ltd.

KEY WORDS: seismic motion; vehicle model; seismic response analysis; vehicle response; expressways

INTRODUCTION

After the 1995 Kobe earthquake, higher priority has been given for the countermeasures against earthquakes than before in Japan. With good financing, thousands of strong motion seismometers were installed in Japan. A number of damage assessment systems were also developed by different organizations [1]. Under this situation, Japan Highway Public Corporation (JH) has developed the new seismometer network along the expressways. Using earthquake information from these instruments, JH closes the expressways if the Peak Ground Acceleration (PGA) is larger than or equal to 80 cm/s^2 [2]. However, recent studies on earthquake

* Correspondence to: Yoshihisa Maruyama, Yamazaki Laboratory, Institute of Industrial Science, The University of Tokyo, 4-6-1 Komaba, Meguro-ku, Tokyo 153-8505, Japan.
† E-mail: maruyama@rattle.iis.u-tokyo.ac.jp

Received 6 December 2001
Revised 19 February 2002
Accepted 20 February 2002

damage have revealed that expressway structures are not seriously damaged under such level of seismic motion [3]. Though JH closes the expressways under this ground motion level, the serious damages that affect safety driving on expressways are seldom found in the recent years. Hence, we may think of relaxing the regulation of expressway closure.

In this objective, we need to examine the effects of seismic motion to the automobile drivers on expressways since they may encounter difficulties in keeping safety driving and traffic accidents may occur. In fact, some drivers who have experienced the Kobe earthquake on the expressways reported that controlling their vehicles was almost impossible during strong shaking. Generally, under a large seismic motion, we feel some difficulties to continue doing something that is easily done in the ordinary time, for instance, operating a control system in nuclear power plants. Shibata *et al.* [4] tested the accuracy of typing under the strong motion using a computer set on a two-dimensional shaking table. In nuclear power plants, a power generation system is controlled by computers, and if a large earthquake occurs, operators have to stop the system immediately. They may feel some difficulties in operating the keyboard and switching of the system under intense shaking.

Yamanouchi and Yamazaki [5] investigated drivers' response to strong seismic motion using a driving game machine set on a shaking table. However, the driving game machine used in this experiment had lack of reality as it was made for amusement purpose. Recently, driving simulators that take into account vehicle dynamics are introduced to several organizations [6]. In 1999, the driving simulator with six servomotor-powered electric actuators was introduced to the Institute of Industrial Science, the University of Tokyo [7]. Using this driving simulator, we can conduct a series of virtual tests to clarify drivers' responses and their feelings while controlling the simulator under various seismic motions with good reality. Before doing this, we need to investigate the response characteristics of an automobile under various seismic excitations.

In this study, a vehicle was modelled with a six-degree-of-freedom system and its responses under several seismic motions were evaluated. Based on the obtained results, the effects of seismic motion to the dynamic response of a vehicle were investigated, and these response characteristics may be useful for decision-making regarding the expressway closure under seismic motion.

A VEHICLE MODEL WITH SIX DEGREES-OF-FREEDOM

We define three axes set on the centre of gravity (c.g.) of a vehicle. The x-axis is the longitudinal direction, the y-axis is the transverse direction, and the z-axis is the vertical direction of the vehicle [8]. Figure 1 shows the fundamental motions of a vehicle. The model has three translation motions (longitudinal, transverse and vertical) and three rotational motions (rolling, pitching and yawing). Figure 2 shows the two-dimensional coordinate for describing these motions on the X–Y plane. In this figure, the X–Y coordinate (the absolute coordinate) is independent of the position of the vehicle. The equations of motion of the vehicle to the longitudinal and transverse directions are defined as

$$m(\dot{u} - vr) = \sum_i \sum_j (F_{xij} \cos \delta_{tij} - F_{yij} \sin \delta_{tij}) = \sum_{i,j} F'_{xij} \tag{1a}$$

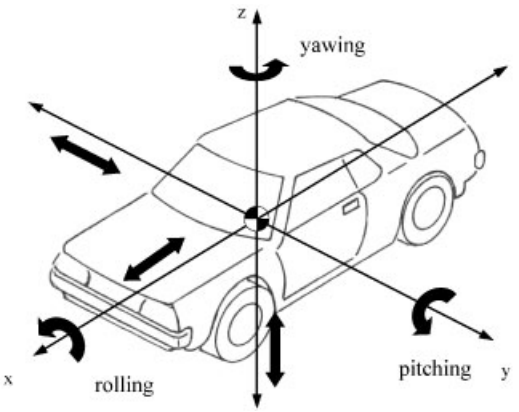

Figure 1. Fundamental motions of a vehicle.

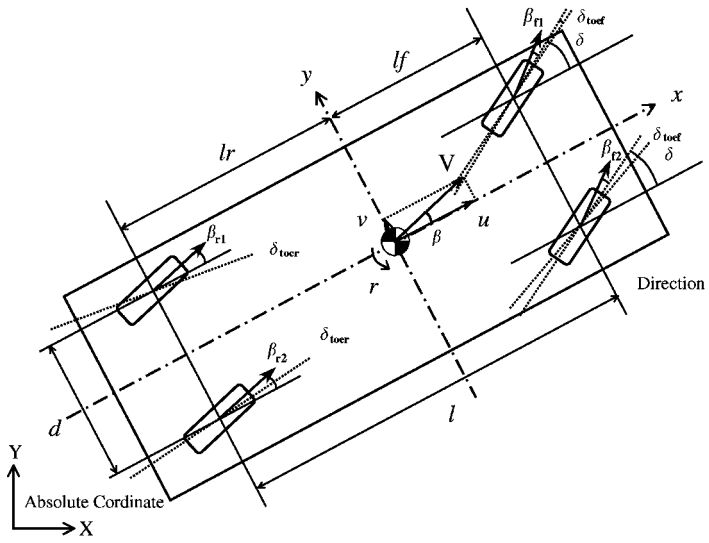

Figure 2. Two-dimensional coordinate of vehicle motion on X–Y plane.

$$m(\dot{v} + ur) = \sum_i \sum_j (F_{xij} \sin \delta_{tij} + F_{yij} \cos \delta_{tij}) = \sum_{i,j} F'_{yij} \tag{1b}$$

where u and v are the velocities in the x and y directions, respectively, r is the angular velocity of yawing, δ is the angle difference between the x-direction and the direction of each tyre, F_x and F_y are the longitudinal and transverse forces of each tyre, respectively. The index i represents the front or rear wheel and the index j represents the left or right wheel.

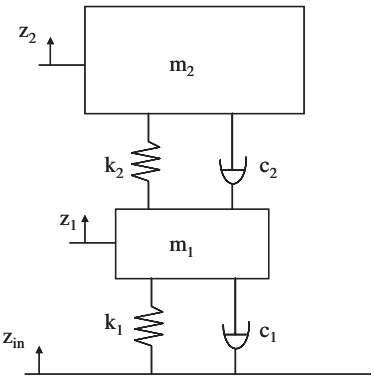

Figure 3. Quarter vehicle model for vertical motion.

The yawing motion is defined as

$$I_z \frac{\mathrm{d}r}{\mathrm{d}t} = (F'_{y11} + F'_{y12})l_\mathrm{f} - (F'_{y21} + F'_{y22})l_\mathrm{r} + (-F'_{x11} + F'_{x12})\frac{d}{2} + (-F'_{x21} + F'_{x22})\frac{d}{2} \tag{2}$$

where I_z is the mass moment of inertia of the vehicle about the z-axis, l_f and l_r are the distance between the c.g. and the front wheel and that between the c.g. and the rear wheel, respectively, and d is the distance between the right and left wheels. Rolling (ϕ), yawing (ψ) and pitching (θ) angles are defined by Equations (3), (4) and (5), respectively.

$$(K_\phi - mgh)\phi = m(\dot{v} + ur)h \tag{3}$$

$$\psi = \int r \, \mathrm{d}t \tag{4}$$

$$\{2K(l_\mathrm{f}^2 + l_\mathrm{r}^2)\}\theta = m(\dot{u} - vr)h \tag{5}$$

where K_ϕ is the rolling stiffness, K is the spring constant of the suspension, and h is the height of the c.g..

From Equations (1)–(5), the motions of the vehicle are described in the x–y coordinate system, set on the c.g. of the vehicle. The velocities in the absolute coordinate can be defined as

$$\dot{X} = u \cos \psi - v \sin \psi \tag{6a}$$

$$\dot{Y} = u \sin \psi + v \cos \psi \tag{6b}$$

So far, we have described the five kinds of motions out of six. The last one is the vertical motion. In order to describe vertical motion, a quarter vehicle model (Figure 3) is employed [8]. The upper mass represents the body of a vehicle and the lower mass represents a tyre. The upper spring is the suspension of the vehicle and the lower spring represents the stiffness of

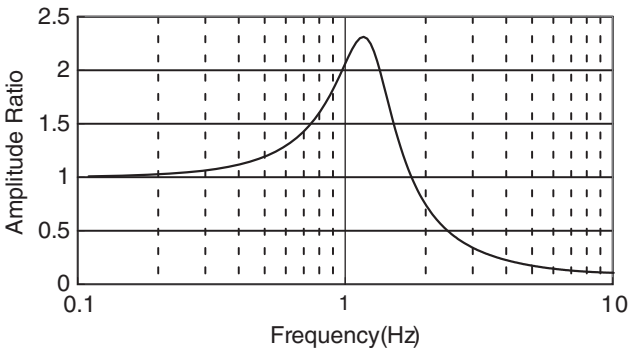

Figure 4. Transfer function of the vehicle model to vertical motion.

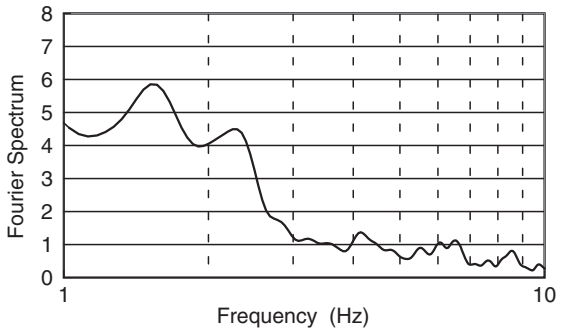

Figure 5. Measured velocity Fourier spectrum of the vertical component when an actual car was running.

the tyre. According to this model, the equation of motion to the vertical direction is described as

$$m_1(\ddot{\zeta}_1 + \ddot{z}_{in}) + c_1\dot{\zeta}_1 + c_2(\dot{\zeta}_1 - \dot{\zeta}_2) + k_1\zeta_1 + k_2(\zeta_1 - \zeta_2) = 0 \tag{7a}$$

$$m_2(\ddot{\zeta}_2 + \ddot{z}_{in}) + c_2(\dot{\zeta}_2 - \dot{\zeta}_1) + k_2(\zeta_2 - \zeta_1) = 0 \tag{7b}$$

where z_{in} is the vertical displacement of the ground $\zeta_1(=z_1 - z_{in})$ and $\zeta_2(=z_2 - z_{in})$ are the relative vertical displacements of m_1 and m_2, respectively.

Substituting the respective parameters to Equation (7), the transfer function between z_{in} and z_2 can be derived. The transfer function obtained in this study is shown in Figure 4. The predominant frequency is observed at around 1.2 Hz. In order to examine this modelling, the measurements of acceleration were conducted using an actual car (Honda Civic) while it was running. The calculated velocity Fourier spectrum for the vertical component is shown in Figure 5. In the figure, the predominant frequency is observed at around 1.5 Hz, however, this characteristic is dependent on type of car.

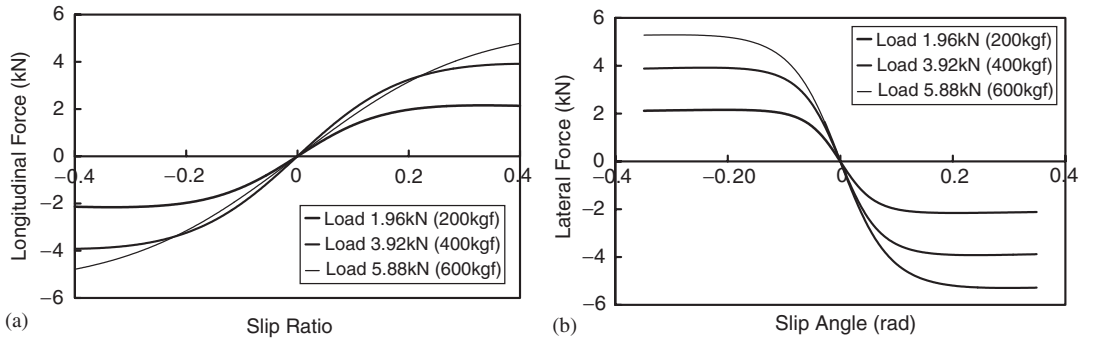

Figure 6. Characteristics of the Magic Formula Model used in this study for (a) the longitudinal force and (b) the lateral force.

SEISMIC RESPONSE ANALYSIS OF THE VEHICLE MODEL

Magic formula model

In order to conduct seismic response analysis of a vehicle, we have to calculate the force acting on each tyre. In this study, the Magic Formula Model (MFM) [9] was employed. Equation (8) shows the fundamental equation used in the MFM. All the coefficients used in this equation are determined empirically by some experiments of the manufacturer of actual driving simulators.

$$y(x) = D \sin[C \arctan\{Bx - E(Bx - \arctan(Bx))\}] \tag{8a}$$

$$Y(x) = y(x) + S_{\mathrm{v}} \tag{8b}$$

$$x = X + S_{\mathrm{h}} \tag{8c}$$

where B, C, D and E are the stiffness, shape, peak and curvature factors, respectively, and S_{h} and S_{v} are the amount of the horizontal and vertical shifts, respectively. In the model used in this study, both the shifts are set equal to zero.

$Y(x)$ in Equation (8b) is the output force (longitudinal or lateral) of the MFM. For calculating the lateral force, F_y, the slip angle is used as the input value X in Equation (8c). For the longitudinal force, F_x, the slip ratio is used as the input value. In this study, the slip ratio is set equal to zero because it is assumed that the vehicle is running without accelerating or braking. The characteristics of the MFM used in this study are shown in Figure 6.

In order to calculate the lateral force, F_y, B, C and D are derived as

$$BCD_y = a_3 \sin(2 \arctan(W_{\mathrm{t}ij}/a_4)) \tag{9a}$$

$$C_y = 1.3 \tag{9b}$$

$$D_y = (a_1 W_{\mathrm{t}ij} + a_2) W_{\mathrm{t}ij} \tag{9c}$$

$$B_y = BCD_y / C_y / D_y \tag{9d}$$

where W_{tij} is the vertical load of each tyre. F_y is equal to $-Y(x)$ because the lateral force is negative when the slip angle is positive. For the longitudinal force, F_x, B, C and D are derived as

$$BCD_x = (b_3 W_{tij}^2 + b_4 W_{tij}) \exp(-b_5 W_{tij}) \tag{10a}$$

$$C_x = 1.65 \tag{10b}$$

$$D_x = (b_1 W_{tij} + b_2) W_{tij} \tag{10c}$$

$$B_x = BCD_x / C_x / D_x \tag{10d}$$

Seismic response analysis

In order to conduct the seismic response analysis, Equation (1) is modified as

$$m_2(\dot{u} - vr + \ddot{x}\cos\psi + \ddot{y}\sin\psi) = \sum_i \sum_j (F_{xij}\cos\delta_{tij} - F_{yij}\sin\delta_{tij}) = \sum_{i,j} F'_{xij} \tag{11a}$$

$$m_2(\dot{v} + ur - \ddot{x}\sin\psi + \ddot{y}\cos\psi) = \sum_i \sum_j (F_{xij}\sin\delta_{tij} + F_{yij}\cos\delta_{tij}) = \sum_{i,j} F'_{yij} \tag{11b}$$

where $\ddot{x}$ and $\ddot{y}$ are the ground accelerations to the longitudinal and transverse directions of the vehicle, respectively.

For the vertical component, the vertical ground acceleration was substituted as $\ddot{z}_{in}$ in Equation (7). When pitching and rolling motions occur, the vertical load of the tyre will change. The static vertical load of the tyre is described as

$$W_{t0f} = 0.5 m_2 g l_r / (l_f + l_r) + m_1 g/4 \tag{12a}$$

$$W_{t0r} = 0.5 m_2 g l_f / (l_f + l_r) + m_1 g/4 \tag{12b}$$

where f and r represent front and rear, respectively. The change of the vertical load due to pitching and rolling motions can be described as

$$W_{tr} = m_2(\dot{v} + ru)h/d \tag{13a}$$

$$W_{tp} = m_2(\dot{u} - rv)h/(l_f + l_r) \tag{13b}$$

Considering these changes due to pitching and rolling motions, the vertical load of each tyre is described as

$$W_{t11} = W_{t0f} - (W_{tp} + W_{tr})/2 \tag{14a}$$

$$W_{t12} = W_{t0f} - (W_{tp} - W_{tr})/2 \tag{14b}$$

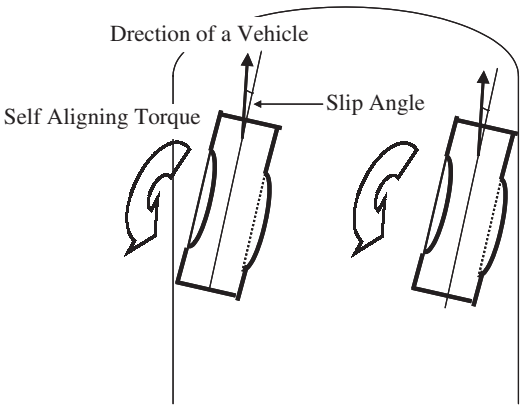

Figure 7. Self-aligning torque acting on each tyre.

$$W_{t21} = W_{t0r} + (W_{tp} - W_{tr})/2 \tag{14c}$$

$$W_{t22} = W_{t0r} + (W_{tp} + W_{tr})/2 \tag{14d}$$

When the vertical motion is considered, the vertical load of each tyre is also changed accordingly. Considering the change of the load due to the vertical motion, the total vertical load of each tyre is described as

$$W_{tij}^{\text{total}} = W_{tij} - (k_1\zeta_1 + c_1\dot{\zeta}_1)/4 \tag{15}$$

The height of the c.g. is also changed when the vertical motion is generated. The height of the c.g. is described as

$$h = h_0 + \zeta_2 \tag{16}$$

where h_0 is the height of the c.g. under the static condition.

The moment called the self-aligning torque shown in Figure 7, which reduces the slip angle of each tyre, is also considered. This moment is expected to reduce the lateral displacement generated by seismic motion. When a tyre generates a lateral force, the point where the force acts is not the centre of the tyre. The length between the centre of the tyre and the point where the force acts is called the pneumatic trail. It is in the range of 1–4 cm, depending on tyres. The self-aligning torque is the product of the pneumatic trail and lateral force. Figure 8 shows the relationship between the slip angle and pneumatic trail and the relationship between the slip angle and self-aligning torque. Using the self-aligning torque, δ (Figure 2) is calculated as

$$\delta = (\text{SAT}_{11} + \text{SAT}_{12})/K_{\text{st}} \tag{17}$$

where SAT is the self-aligning torque and K_{st} is the elastic coefficient of the steering.

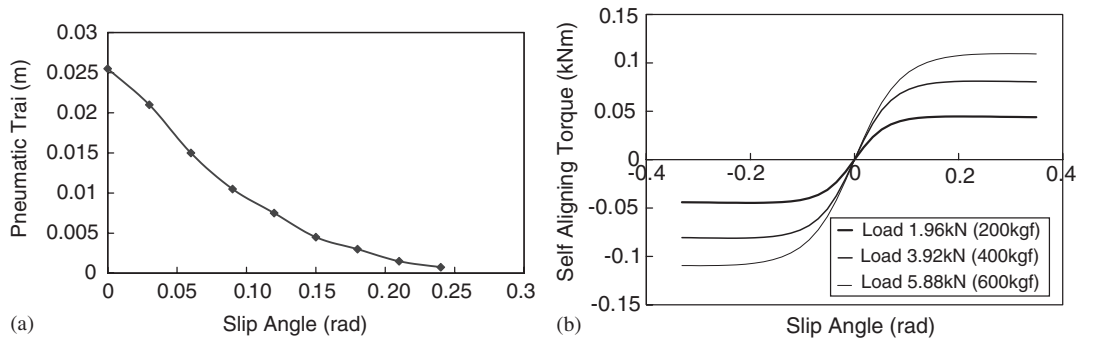

Figure 8. (a) The relationship between the slip angle and pneumatic trail (b) and the relationship between the slip angle and self-aligning torque.

In order to calculate the lateral force and self aligning torque, the slip angle is necessary. The slip angle for each tyre is described as follows:

$$\beta_{11} = (V\beta + l_f r)/(V - \mathrm{d}r/2) - \delta \tag{18a}$$

$$\beta_{12} = (V\beta + l_f r)/(V + \mathrm{d}r/2) - \delta \tag{18b}$$

$$\beta_{21} = (V\beta - l_r r)/(V - \mathrm{d}r/2) \tag{18c}$$

$$\beta_{22} = (V\beta - l_r r)/(V + \mathrm{d}r/2) \tag{18d}$$

where

$$\beta = \arctan(v/|u|) \tag{19a}$$

$$V = \sqrt{u^2 + v^2} \tag{19b}$$

As $|\beta|$, $|l_f r/V|$, $|l_r r/V|$, and $|\mathrm{d}r/2V|$ are much smaller than 1, Equation (18) can be approximated as

$$\beta_f \approx \beta + l_f r/V - \delta \tag{20a}$$

$$\beta_r \approx \beta - l_r r/V \tag{20b}$$

where β_f is the slip angle of the front wheels and β_r is that of the rear wheels.

Table I shows the parameters of the vehicle model used in this study. All parameters are set to be the same as those used in the driving simulator developed by Mitsubishi Precision Co., Ltd. However, this driving simulator does not deal with the vertical motion. The proper parameters for the vertical motion were adopted from Reference [8]. This vehicle model is designed for a compact car.

Table I. Parameters of the vehicle model used in this study.

Parameters	Definition	Value	Unit
m_2	Mass of the vehicle body	1100	kg
l_f	Length between the centre of gravity and the front wheel	1.0	m
l_r	Length between the centre of gravity and the rear wheel	1.635	m
I_z	Inertial moment for yawing motion	637	kg m^2
h_0	Height of the centre of gravity under static condition	0.35	m
d	Length between right and left wheels	1.505	m
K_ϕ	Stiffness for rolling motion	117.6	kN m
K_{st}	Elastic constant of the steering	48.5	kN m/rad
m_1	Mass of the wheels*	100	kg
k_1	Spring constant of the tyres†	784	kN/m
k_2	Spring constant of the suspension‡	68.6	kN/m
c_1	Coefficient of viscosity of the tyres§	98	N s/m
c_2	Coefficient of viscosity of the suspension	4.9	kN s/m
a_1	Coefficient of the Magic Formula Model	−0.0005	—
a_2	Coefficient of the Magic Formula Model	1.2	—
a_3	Coefficient of the Magic Formula Model	6256.0	—
a_4	Coefficient of the Magic Formula Model	612.0	—
b_1	Coefficient of the Magic Formula Model	−0.0005	—
b_2	Coefficient of the Magic Formula Model	1.2	—
b_3	Coefficient of the Magic Formula Model	0.1	—
b_4	Coefficient of the Magic Formula Model	0.8	—
b_5	Coefficient of the Magic Formula Model	0.005	—

* Mass for 4 wheels.
† Spring constant for 4 tyres.
‡ Spring constant for 4 suspensions.
§ Coefficient of viscosity for 4 tyres.

Before conducting a seismic response analysis, the response characteristics of this vehicle model were investigated. The sinusoidal wave with a certain frequency was applied to the transverse direction of the vehicle model and then the absolute response acceleration to the transverse direction was calculated. Figure 9 shows the amplitude ratio and phase delay between the input and response accelerations. In the figure, when the frequency of the input motion is low, the amplitude ratio between the input and response accelerations is close to 1.0. For higher frequencies, the model shows smaller amplitude ratios and larger phase delays.

A seismic response analysis is performed using five actual earthquake records. The records used in this study are the Kobe Marine Observatory of Japan Meteorological Agency (JMA) of the 1995 Kobe earthquake, the El Centro of the 1940 Imperial Valley earthquake [10], the K-NET [11] Kofu of the 2000 Tottori-ken Seibu earthquake, SCT of the 1985 Mexico earthquake [10], and the Chiba Experiment Station of the Institute of Industrial Science, the University of Tokyo of the 1987 Chiba-ken Toho-Oki earthquake [12].

Figure 10 shows the acceleration time histories (the transverse component to the vehicle) used in this study. Considering the sensitivity of the model (Figure 9), the filtered motions with the range of 0.2–10 Hz were employed as input motions. Figure 11 shows the acceleration response spectra with 5% damping ratio for the records (the transverse component to the vehicle) scaled to PGA equal to 300 cm/s^2. The acceleration response spectrum of the SCT,

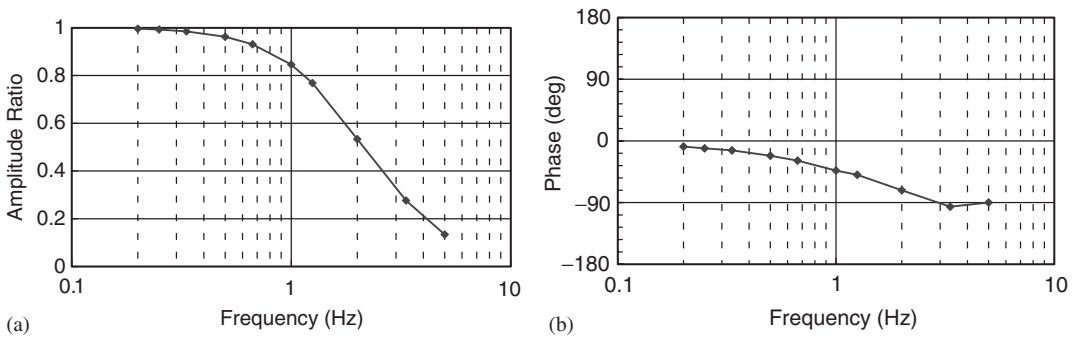

Figure 9. (a) Amplitude ratio and (b) phase delay between input and response accelerations under harmonic excitation.

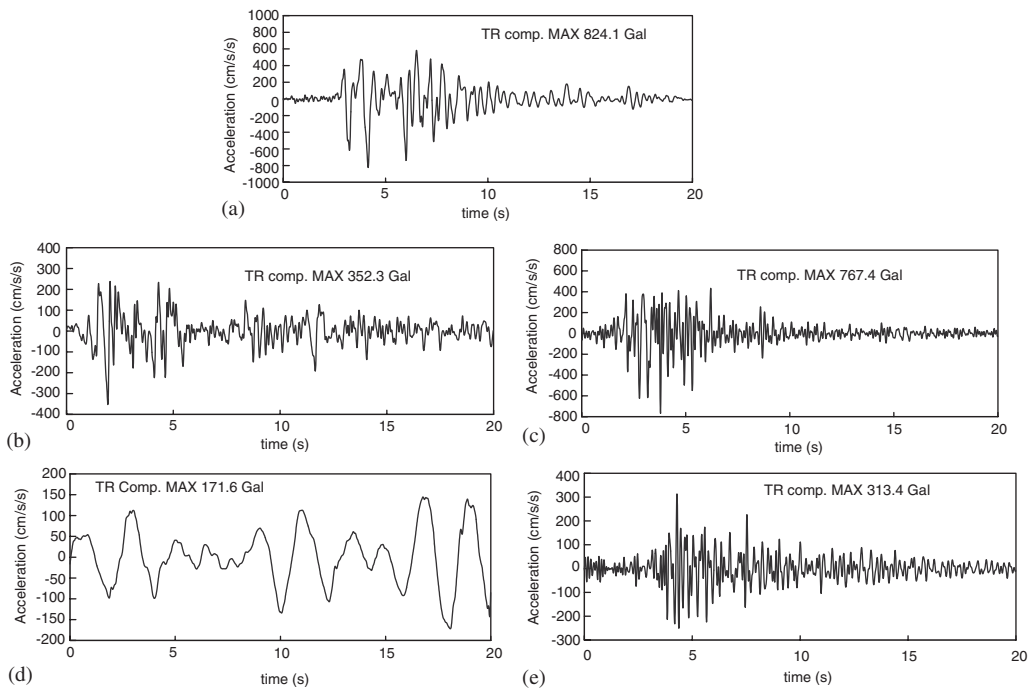

Figure 10. Acceleration time histories applied to the transverse direction of the vehicle model, recorded at (a) JMA Kobe, (b) El Centro, (c) K-NET Kofu, Tottori, (d) SCT Mexico, and (e) Chiba Experiment Station.

Mexico record has much larger value in the frequency range smaller than 1 Hz compared with those of the other records. It is also observed that the acceleration response spectra of the El Centro and JMA Kobe records are larger than those of the Tottori and Chiba records in the frequency range smaller than 2 Hz.

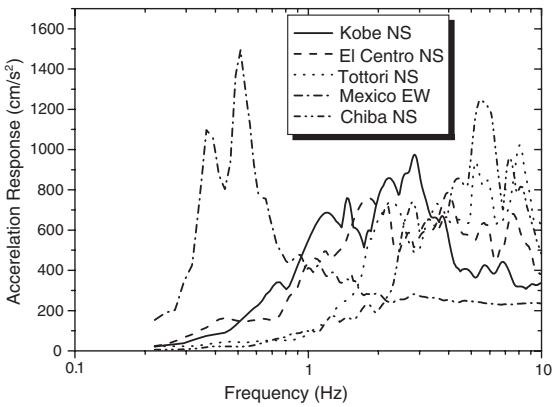

Figure 11. Acceleration response spectra with 5% damping ratio of five records scaled to PGA = 300 cm/s^2, applied to the transverse direction of the vehicle.

In order to apply seismic motion to the vehicle model, the recorded seismic motions were scaled with respect to PGA. The three-component seismic record was applied to the vehicle model, in each case by scaling the record with respect to the PGA of the transverse component. The running speed of a vehicle was set to be 100 km/h. This is the maximum speed limit of the expressways in Japan by law.

Figure 12 shows the response of the vehicle subjected to the seismic motion scaled to 800 cm/s^2 except the Mexico record, which was scaled to 300 cm/s^2. The relative lateral displacement is an important index to realize whether the vehicle protrudes from its running lane or not. In order to calculate the relative lateral displacement of the vehicle to the ground, the relative velocity of the vehicle to the ground, v, and the yaw angle, ψ, which can be derived by integrating yaw angular velocity, r, are also important factors (Equation (6)). In this study, as the indices representing the vehicle responses to seismic excitation, the relative lateral velocity, yaw angular velocity, and relative lateral displacement were selected. It is observed in the figure that the responses of the vehicle to the El Centro and Kobe records are larger than those to the Tottori and Chiba records even though all the records were scaled to have the same PGA value. Although the Mexico record was scaled to have the smallest PGA value, the response of the vehicle to the Mexico record is rather large. This is mainly because of the characteristics of the vehicle response (Figure 9) and the acceleration response spectrum (Figure 11). The vehicle model has high amplitude ratios in the smaller frequency range and the Mexico record has large spectral acceleration in this range. The relative lateral displacement of the vehicle does not become zero but shows almost a straight line of increasing trend. This means that the vehicle has a non-zero yaw angle after the main part of the earthquake input motion.

Figures 13 and 14 show the relationship between the PGA and the maximum relative lateral velocity and yaw angular velocity for the five input motions. The running speed of the vehicle was set as 100 and 120 km/h, respectively. These relationships are almost linear and the variation is observed from event to event even the same PGA value was applied. The Mexico record was associated by larger relative lateral velocity responses compared with those of the other four records, and the Mexico record showed much larger yaw angular

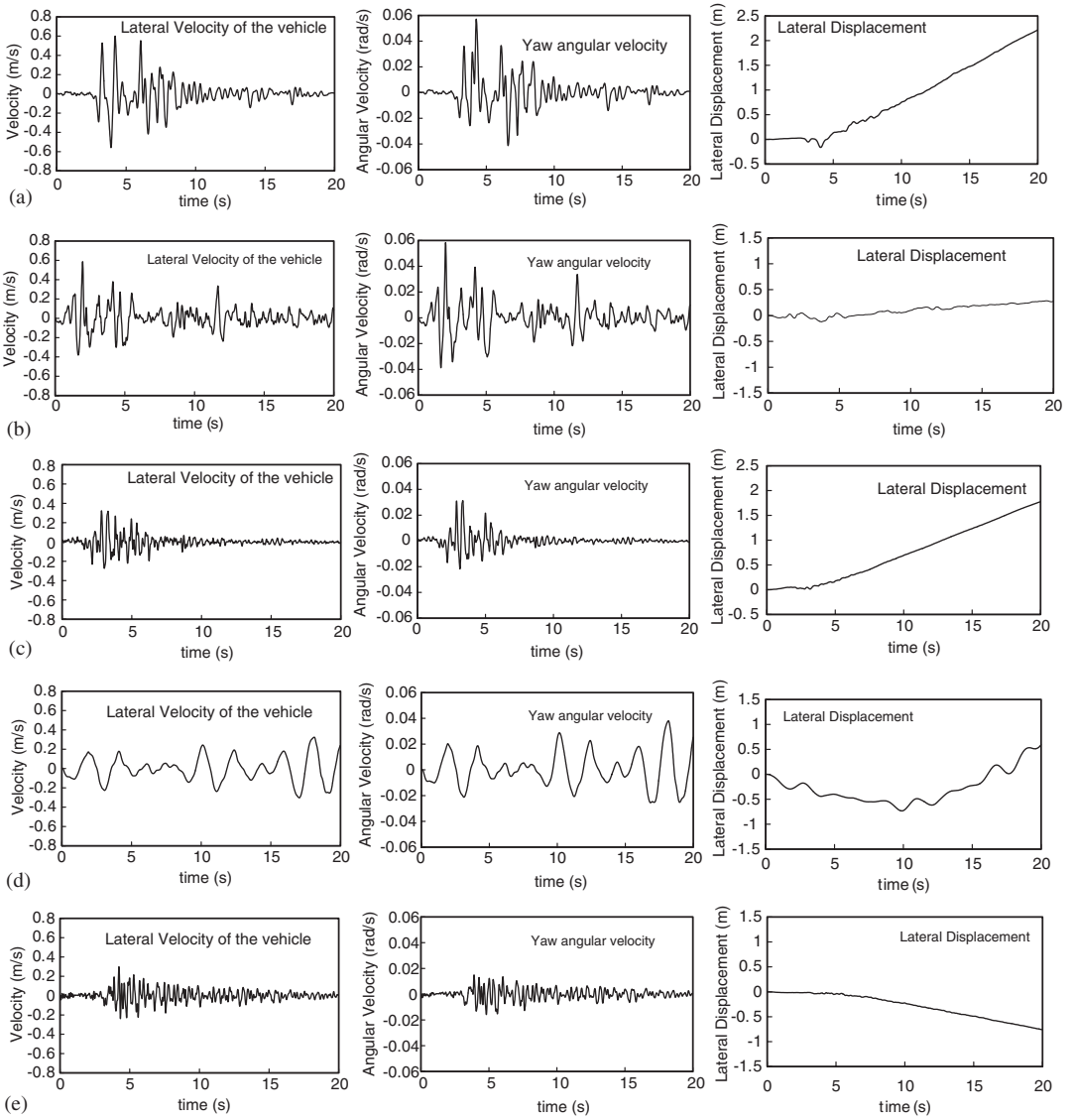

Figure 12. Dynamic responses of the vehicle due to seismic motions recorded at (a) JMA Kobe, (b) El Centro, (c) K-NET Kofu, Tottori, (d) SCT Mexico and (e) Chiba Experiment Station. Those records were scaled to PGA = 800 cm/s^2 (only for Mexico record, scaled to 300 cm/s^2). The initial running speed of the vehicle was set as 100 km/h.

velocity responses than that of other records. It is also observed that, as the running speed of the vehicle becomes larger, the vehicle response also becomes a little larger accordingly.

Figure 15 shows the relationship between the PGV and the maximum relative lateral velocity and yaw angular velocity for the five input motions. It is observed (Figure 15) that the

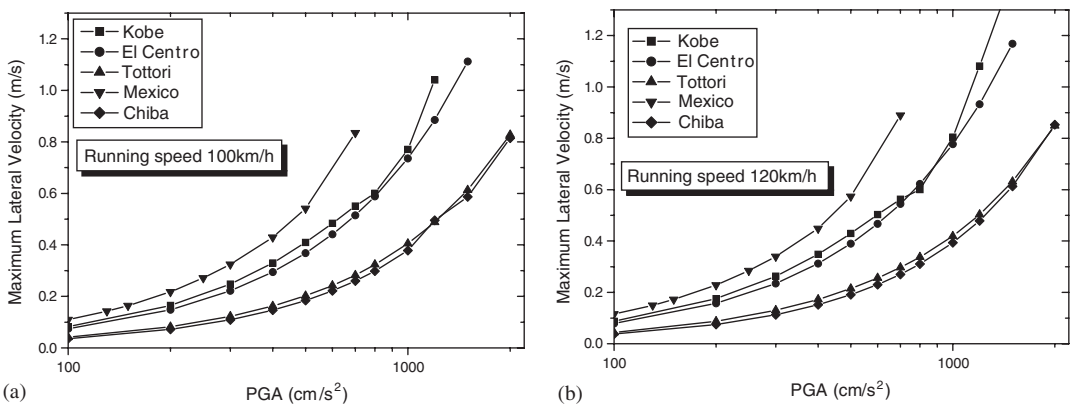

Figure 13. Relationship between the maximum relative lateral velocity and peak ground acceleration applied to the transverse direction to the vehicle. The initial running speed of the vehicle was set as (a) 100 km/h and (b) 120 km/h.

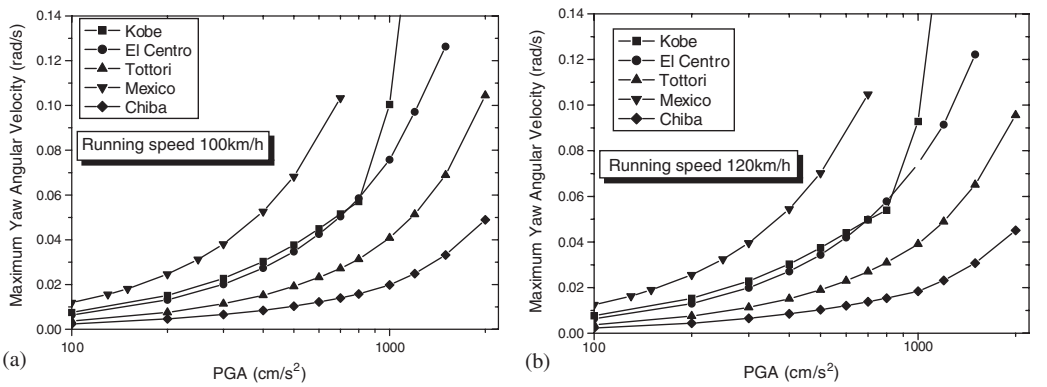

Figure 14. Relationship between the maximum yaw angular velocity and peak ground acceleration applied to the transverse direction to the vehicle. The initial running speed of the vehicle was set as (a) 100 km/h and (b) 120 km/h.

variations of the maximum values of the relative lateral velocity and yaw angular velocity are not so large from event to event except for the response under the Mexico record. It should be noted (Figure 15) that the Mexico record looks quite different from the other seismic records. When plotting the vehicle responses as a function of input PGV, the input acceleration of the Mexico record is much smaller than those of the other records. Hence, it is difficult to express various characteristics of seismic motion using only one strong motion index. Except for the Mexico record, which contains long period contents, however, the PGV still seems to be a good index to express ground motion severity from the viewpoint of vehicle response. Figure 16 shows the relationship between the maximum response of the vehicle and JMA

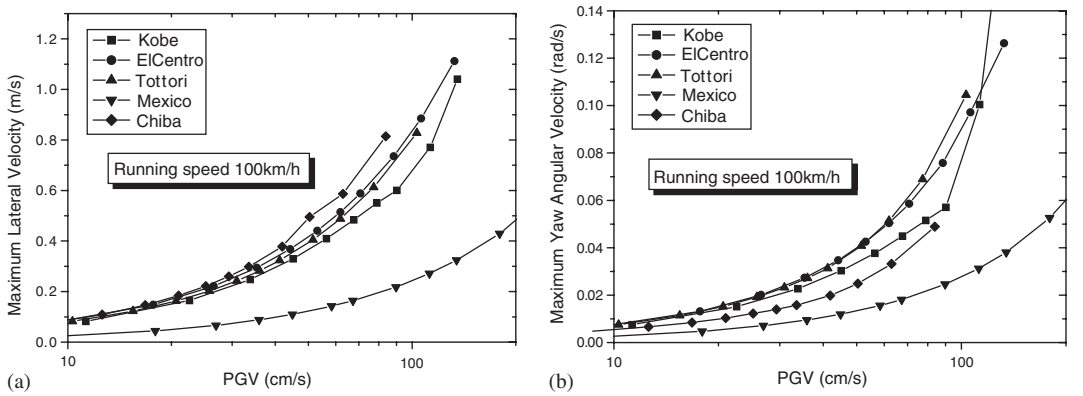

Figure 15. (a) Relationship between the maximum relative lateral velocity of the vehicle and the peak ground velocity applied to the transverse direction of the vehicle and (b) the relationship between the maximum yaw angular velocity of the vehicle and the peak ground velocity, both for the initial running speed of 100 km/h.

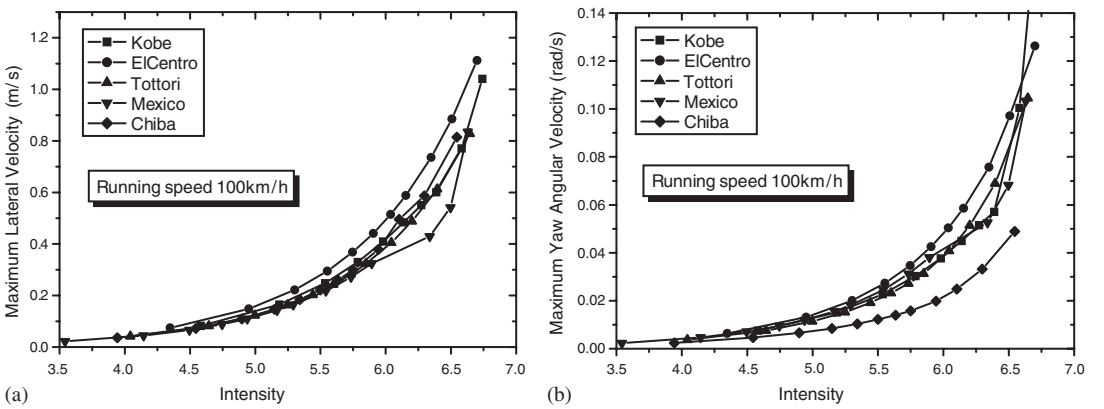

Figure 16. (a) Relationship between the maximum relative lateral velocity of the vehicle and the JMA seismic intensity and (b) the relationship between the maximum yaw angular velocity of the vehicle and the JMA seismic intensity, both for the initial running speed of 100 km/h.

instrumental seismic intensity [13, 14]. In this case, it can be seen that the variations of the responses are very small including the response of the Mexico record.

So far, the relative responses are discussed from the viewpoint of the stability of an automobile without driver's reactions. For drivers, the absolute response acceleration of the vehicle affects the stability of controlling the vehicle. The absolute response acceleration is described as

$$\mathrm{AbsAcc}_{\mathrm{LT}} = \dot{u} - vr + \ddot{x}\cos\psi + \ddot{y}\sin\psi \tag{21a}$$

$$\mathrm{AbsAcc}_{\mathrm{TR}} = \dot{v} + ur - \ddot{x}\sin\psi + \ddot{y}\cos\psi \tag{21b}$$

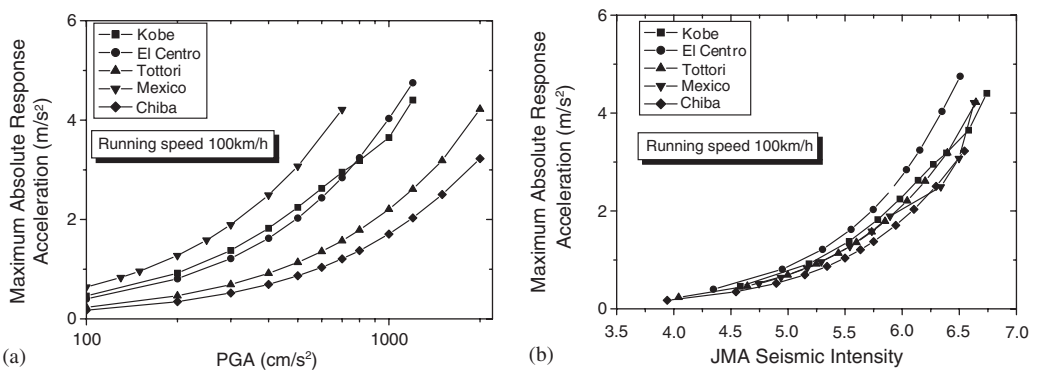

Figure 17. (a) Relationship between the maximum absolute response acceleration of the vehicle and the peak ground acceleration to the transverse direction and (b) relationship between the maximum absolute response acceleration of the vehicle and the JMA seismic intensity of the input ground motion.

where $\mathrm{AbsAcc_{LT}}$ and $\mathrm{AbsAcc_{TR}}$ are the absolute accelerations to the longitudinal and transverse directions, respectively. Figure 17 shows the relationship between the PGA and maximum absolute response acceleration and the relationship between the JMA seismic intensity and maximum absolute response acceleration. In the figure, the variation is seen from event to event with respect to the PGA, however, the variation is not seen with respect to the JMA seismic intensity. The JMA seismic intensity is calculated through a frequency filtering of a three-component record. This process may have similarity with the response characteristics of the vehicle model used in this study.

Based on all these results, the JMA seismic intensity may be the most suitable index to express the severity of seismic motion from the viewpoint of vehicle responses. However, it is necessary to consider wider variations of input motions and vehicle parameters to draw a solid conclusion for which a further study is necessary.

FURTHER STUDY USING DRIVING SIMULATOR

As shown in Figure 12, in many cases the relative lateral displacement does not become zero after the main shaking part of an earthquake input motion. This is because, in the seismic response analysis, the reactions of the driver during shaking are not considered. Regarding the results of Figure 12, the lateral displacement would seem to pose the greatest danger if allowed to develop as shown; however, due to the rather long time for it to develop, driver's reaction should be able to prevent such large drifts from occurring. Also there is the possibility that the driver may produce much larger lateral drifts because of the overreaction to the seismically induced vehicle motions. To deal with this issue in more accurate manner, the reactions of drivers should be taken into account in calculation although it is by no means an easy task. In order to investigate and clarify the drivers' responses under seismic motion, driving simulators, which are newly developed considering vehicle dynamics, may be helpful [7].

A driving simulator was introduced to the Institute of Industrial Science, the University of Tokyo. A scenario highway course is equipped with the simulator for virtual driving. The front view from the driver's seat is realized by three large screens with LCD projectors. The sound system and mirrors give good reality to the simulator. This simulator has six servomotor-powered electric actuators to simulate the motion of a vehicle. Originally, this simulator was designed to simulate the acceleration while driving a vehicle. The control system of the driving simulator was recently modified such that the response of a vehicle due to seismic motion can be applied through the actuators.

Experiments using this driving simulator can evaluate human reaction to seismic motion properly. We are currently conducting such experiments and they are expected to give us useful information on the effects of shaking while driving automobiles in high speed. The results of the virtual experiments will be reported in the near future.

CONCLUSIONS

In order to investigate the response of automobiles subjected to seismic motion, a vehicle model with six degrees of freedom was developed and the seismic response analysis of a running vehicle was carried out. The seismic response analyses were conducted using five actual earthquake records. The earthquake motions selected in this study were recorded at JMA Kobe Marine Observatory of the 1995 Kobe earthquake, at El Centro station of the 1940 Imperial Valley earthquake, at K-NET Kofu station of the 2000 Tottori-ken Seibu earthquake, at SCT station of the 1985 Mexico earthquake, and at Chiba Experiment Station of the 1987 Chiba-ken Toho-Oki earthquake.

The vehicle responses for the different input motions were obtained as a function of PGA, PGV, and JMA seismic intensity. The Mexico record showed a larger relative lateral velocity response compared with those of the other four records, and it showed much larger yaw angular velocity response than that of the other records though all records were scaled to have the same PGA value. Since the Mexico record has larger response spectrum amplitudes in the long period range compared with the other records, the response of the vehicle model became larger. However, the vehicle responses for the different input motions showed a very similarity with respect to JMA seismic intensity.

In this study, the absolute response of a vehicle that should affect the vehicle control by a driver was also investigated. When the relationship between the PGA and maximum absolute response acceleration was considered, the variation was seen from event to event. However the variation for the different events was not seen with respect to the JMA seismic intensity.

According to these results, the JMA intensity may be the most suitable index to express the severity of seismic motion from the viewpoint of vehicle responses. However, a further study that considers wider variations in input motion and vehicle parameters may be necessary before the conclusive observation is obtained.

In order to evaluate drivers' responses when seismic motion is subjected, we are currently conducting a series of virtual tests using a driving simulator. These experiments will provide useful information for the promotion of expressway safety in natural disasters.

REFERENCES

1. Yamazaki F, Meguro K, Noda S. Developments of early earthquake damage assessment systems in Japan. *Proceedings of ICOSSAR'97*, Structural Safety and Reliability, 1998; 1573–1580.
2. Maruyama Y, Yamazaki F, Hamada T. Microtremor measurements for the estimation of seismic motion along the expressways. *Proceedings of the Sixth International Conference on Seismic Zonation*, vol. 2, 2000; 1361–1366.
3. Yamazaki F, Motomura H, Hamada T. Damage assessment of expressway networks in Japan based on seismic monitoring. *Proceedings of the 12th World Conference on Earthquake Engineering*, 2000; CD-ROM.
4. Shibata H, Ishibatake H, Fukuda T, Komine H. Human operability under strong earthquake condition. *Proceedings of the Eighth World Conference on Earthquake Engineering*, 1984; 1109–1116.
5. Yamanouchi H, Yamazaki F. Experiments on the behavior of automobile drivers under seismic motion using driving simulator. *Proceedings of the Fifth U.S. Conference on Lifeline Earthquake Engineering*, 1999; 8–16.
6. Hiramatsu K, Satoh K, Uno H, Soma H. The first step of motion systems realization in the JARI driving simulator. *Proceedings of the International Symposium on Advanced Vehicle Control*, 1994; 99–104.
7. Yamazaki F. Seismic monitoring and early damage assessment systems in Japan. *Progress in Structural Engineering and Materials* 2001; **3**:66–75.
8. Ellis JR. *Vehicle Dynamics*. London Business Books Ltd, London, 1969.
9. Bakker E, Pacejka HB, Linder L. A new tyre model with an application in vehicle dynamics studies. *Society of Automotive Engineers (SAE) Paper* No. 890087, 1989.
10. National Oceanic and Atmospheric Administration. *Earthquake Strong Motion CD-ROM*. National Geophysical Data Center: Boulder CO, 1989.
11. Kinoshita S. Kyoshin net (K-NET). *Seismological Research Letters* 1996; **66**:841–844.
12. Katayama T, Yamazaki F, Nagata S, Lu L, Turker T. A strong motion database for the Chiba seismometer array and its engineering analysis. *Earthquake Engineering and Structural Dynamics* 1990; **19**:1089–1106.
13. Shabestari KT, Yamazaki F. Attenuation relationship of JMA seismic intensity using JMA records. *Proceedings of the 10th Japan Earthquake Engineering Symposium*, 1998; 529–534.
14. Karim KR., Yamazaki F, Correlation of JMA instrumental seismic intensity with strong motion parameters. *Earthquake Engineering and Structural Dynamics* 2002; **31**:1191–1212.

